AIMS Materials Science, 5 (5): 932–944.
DOI: 10.3934/matersci.2018.5.932
Received: 23 June 2018
Accepted: 11 September 2018
Published: 26 September 2018

http://www.aimspress.com/journal/Materials

Research article

Enhancement of anticorrosion properties of stainless steel 304L using nanostructured ZnO thin films

Muhamed Shajudheen V P[1,*], Saravana Kumar S[2], Senthil Kumar V[1], Uma Maheswari A[3], Sivakumar M[3] and Sreedevi R Mohan[3]

[1] Department of Physics, Karpagam University, Coimbatore, Tamil Nadu, India
[2] Department of Physics, NSS College Pandalam, Kerala, India
[3] Department of Sciences, Amrita School of Engineering, Coimbatore, Tamil Nadu, India

* **Correspondence:** Email: shajuvp099@gmail.com.

Abstract: Nanostructured ZnO thin films were coated on stainless steel specimen (304L SS) by depositing nanoparticles of zinc oxide. The morphology and optical properties of the thin films were epitomized using Field Emission Scanning Electron Microscopy (FESEM), Energy Dispersive Analysis of X ray (EDAX), Atomic Force Microscopy (AFM) and Photoluminescence spectroscopy (PL) techniques. FESEM and AFM images revealed that the present depositing procedure is extremely proficient to synthesize uniform and homogeneous nanostructured thin films. The presence of excitonic peak in the PL emission spectrum confirmed the nanocrystalline nature of the thin films. The anticorrosion nature of the zinc oxide coated stainless substrate in the brackish environment was studied using Tafel, Electrochemical Impedance Spectroscopy analysis and Open Circuit Potential studies (OCP) methods. The E_{corr}, I_{corr}, corrosion rate before and after salt spray were calculated from Tafel plot. These parameters indicated that the anticorrosion properties of coated thin films are substantially higher to that of bare steel. The Nyquist plot before and after salt spray was fitted using an equivalent circuit and the coating resistance R_{ct} was calculated. The different mechanisms involved in the corrosion behavior of the thin films were discussed on the basis of equivalent circuit. The physical stability of the coated samples in saline surroundings was studied by AFM assisted nanoindentation techniques. The absence of the cracks and blisters in the sample after nanoindentation before and after salt spray revealed the adherent nature of the nanostructured thin films.

Keywords: zinc oxide thin film; spray pyrolysis technique; electrochemical impedance studies; anticorrosion studies; Tafel analysis

1. Introduction

Nanomaterials of transition metal oxides have been in limelight due to their versatile applications in various fields of science and technology. Nanostructured materials of metal oxides such as quantum dots, quantum wires, thin films etc find a wide range of applications. Among the various metal oxides, Zinc oxide is considered to be one of the promising inexpensive wide band gap (3.2 eV) n-type semiconductor oxides with excellent substrate adherence and good electrical conductivity. Nanostructured zinc oxide materials have been used in various applications such as optoelectronic devices, thin film gas sensors, ultrasonic oscillators, liquid crystal displays, transparent electrodes, heat mirrors, photovoltaic devices, multilayer photo thermal conversion system [1–6].

In recent years, the preparation of zinc oxide thin films have been emerged great interest due to their chemical and mechanical stability [7–9]. The corrosion resistances of the metals have been substantially enhanced by the deposition of nanocrystalline and nanocomposite thin films on the surface [10–16]. The nanostructured ZnO thin films deposited on the specimen offer higher wear resistance and corrosion resistance by forming a molecular layer on the surface [17–20]. The deposition of the white rust is blocked by developing a obstacle between the specimen and corrosion medium [18].

Various coating techniques have been used to fabricate zinc oxide thin films including magnetron sputtering, chemical vapour deposition, sol-gel, vacuum arc deposition, molecular beam epitaxy, pulsed laser deposition, reactive evaporation [18,21–28]. These coating techniques have inherent disadvantages such as requirement of high vacuum, high cost per cm^2 lower area coverage etc. Spray pyrolysis is an alternative technique for coating, which is simple, less expensive, large area coverage, reproducible and efficient. However it is difficult to control the size and phase of the nanoparticles coated on the thin film. Also, in the spray pyrolysis method, the oxidation takes place on the surface of the substrate which requires a temperature not less than 300 ºC but the steel substrates will undergo deterioration at a temperature more than 200 ºC [29–31].

In this study, ZnO nanoparticles were prepared by arrested precipitation technique. The as synthesized nanoparticles were dispersed in a solution and were deposited on the steel substrate using spray coating method. The morphology of the thin films was characterized using FESEM and AFM techniques. Photoluminescence techniques were employed to characterize the optical properties. Electrochemical Impedance Spectroscopy analysis (EIS), Tafel and Open Circuit Potential (OCP) analysis were carried out on the thin film to study the anticorrosion properties. The mechanical properties of the coating were studied by AFM assisted nanoindendation method. The corrosion behavior of the thin films in the briny surroundings was analyzed by Tafel, EIS and OCP after 390 hours salt treatment.

2. Experimental

2.1. Specimen preparation

Stainless steel (304L SS) was commercially procured and was cut in various dimensions (50 mm × 10 mm, 20 mm × 10 mm and 10 mm × 10 mm) for coating and further characterization. The substrate surfaces were pretreated using deionized water, acetone and ethanol. The surface layers of the films were etched using an acid solution consisting of sulfuric acid and nitric acid. The substrate surfaces were then treated with glycidoxypropyltrimethoxysilane (GPTMS) solution to improve the adherence nature of the substrates [32]. Zhao et al. reported the adhesion strength of the coatings on substrates by the treatment of GPTMS in the metallic surface has significant influence on the corrosion resistance [33]. The samples were then air dried at 80 ºC for 30 minutes in a hot air oven to remove impurities.

2.2. Spray coating

ZnO Nanoparticles were prepared using arrested chemical precipitation technique [34]. 250 ml deionized water is taken in a beaker and 0.05 gm PVP is added. The solution is stirred for 10 minutes using magnetic stirrer and then added 22.43 gm of $ZnSO_4 \cdot H_2O$ to the solution and stirred continuously for 2 hours. To this solution, 15.5 ml of 2 M NH_4OH is added dropwise while the reactants are continuously stirred till the pH becomes 5.5. After 1 hour reflexing, the precipitate formed is centrifuged, washed several times with water and finally with ethanol, and then air dried to obtain nano powders of zinc hydroxide. The as prepared nanoparticles of ZnOH are annealed at 1000 ºC to obtain nanoparticles of ZnO. Then they were dispersed in a solution containing ethanol, Poly Acrylic Acid (PAA) and Poly Vinyl Alcohol (PVA) and it was stirred for 10 minutes. The solution containing ZnO nanoparticles were spray coated on the substrate using Holmarc Opto-Mechatronics unit. Multiple Beam Interference (MBI) was used to determine the thickness of the thin film samples. The thickness of the ZnO thin film was calculated to be approximately 530 nm.

2.3. Salt spray test

The salt spray test complying ASTM B 117 standards was employed to assess the performance of the thin film coating in saline environment. The specimens of deposited thin films were treated with 3.5% sodium chloride vapours (NaCl) constantly sprayed at 30 ºC for 390 hours.

2.4. Electrochemical measurements

The electrochemical analysis of the nanostructured ZnO thin films were analyzed using electrochemical workstation CH6005D. The ZnO coated thin film, calomel electrode and platinum foil were utilized as working electrode, reference electrode and supplementary electrode respectively. The thin film coating of surface area 1 cm^2 was exposed to 3.5 wt% NaCl at 298 K for corrosion investigation. The polarization plots were measured between 100 KHz to 0.01 Hz at 20 mV/s sweep rate. The E_{corr} values were recorded for a period of 400 minutes with every 30 minutes.

2.5. Morphological and optical characterization

The photoluminescence spectrum of the nanostructured thin films of zinc oxide was characterized using JASCO FP 8200 Spectrofluorometer. The excitation wavelength of the samples was 280 nm. Carl Zeiss Sigma HD FESEM was used to record the FESEM images and EDAX spectrum. NT-MDT Solver 47 Pro system was used to record the AFM images and AFM assisted nanoindentation of the thin film samples.

3. Results and discussion

3.1. FESEM and EDAX studies

Figure 1 shows the FESEM micrograph of zinc oxide thin film deposited on steel substrate by spray coating technique. The average grain size of ZnO in the films is approximately 150 nm. FESEM analysis ascribed that the nanoparticles of ZnO have uniformly deposited over the substrate to obtain a homogeneous thin film. The size of the pores in the samples is less than 100 nm and there were no cracks in the film. The chemical constituents of the as prepared zinc oxide thin film calculated from EDAX is shown in the Figure 2. The intense peaks in the EDAX pattern correspond to zinc and oxygen. The compositions of Zn, O are 53.6 and 46.4 atom% respectively. From the EDAX pattern, it can be observed that there were no impurities or traces of the solvent mixture in the nanostructured thin film.

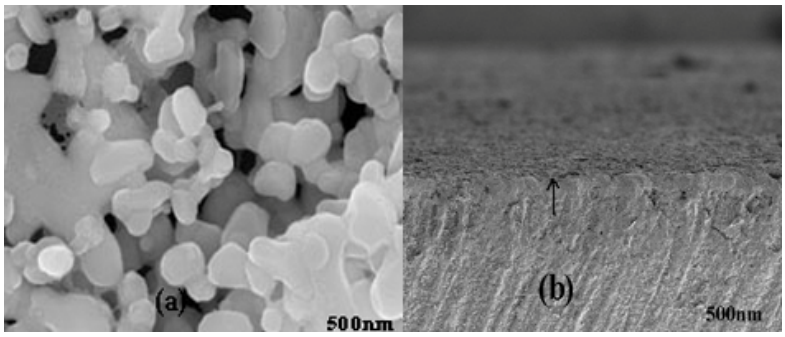

Figure 1. FESEM micrograph of ZnO thin films.

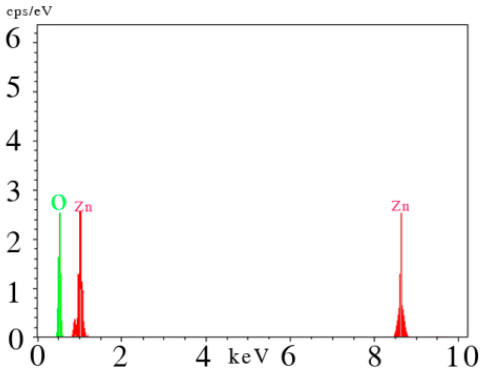

Figure 2. EDAX mapping of ZnO thin films.

3.2. Photoluminescence studies

Figure 3 represents the room temperature photoluminescence spectrum of zinc oxide thin films excited at 350 nm. The PL spectrum of ZnO may consist of two types of peaks, defect related emission as well as near band edge UV emission. The PL spectrum of the present sample shows broad emission peaks around 360, 385 and 395 nm. The broad emission peak at 360 nm can be attributed to the free exciton ($1S_e$–$1S_h$) recombination at room temperature. The exciton emission peaks will not be observed around room temperature in the case of bulk ZnO as its exciton binding energy is fewer than that of thermal energy. The presence of emission peak due to exciton recombination in the present study confirms the nanocrystalline nature of the thin films. The peak at 385 nm can be attributed to band edge emission [35–37]. The peak observed at 395 nm may be ascribed to the oxygen vacancy or Zn interstitial related defects [8]. However these peaks may also be ascribed due to interaction effect of interface of interlayer. A detailed study on the PL spectrum is warranted in order to analyse the exact reason for the occurrence of the peaks.

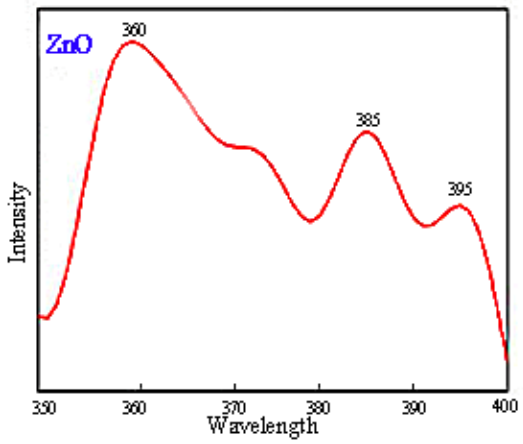

Figure 3. Photoluminescence spectrum of ZnO thin films.

3.3. Tafel studies

Figure 4a shows the Tafel polarization plots of bare steel (304L SS) after 390 h salt spray test. Figures 4b, c shows Tafel polarization plots of ZnO thin films deposited on 304L SS before and after salt spray test. The equilibrium corrosion potential (E_{corr}) of the ZnO films before salt spray test shows about 0.41 V, which is positively shifted compared to that of bare stainless steel (−0.96 V). Hosseini et al. reported the anticorrosion properties of Polypyrrole (PPy) and PPy-ZnO coating on mild steel and observed the incorporation of ZnO nanorods in the PPy coating resulted in the positive shift of E_{corr} value indicating improved corrosion protection [38]. The corrosion parameters E_{corr}, I_{corr} and corrosion rate were calculated by extrapolating Tafel curves and are shown in the Table 1. The shift in (E_{corr}) can be attributed to the improved corrosion resistance of the coated samples. The E_{corr} values of the samples were decreased to 0.25 V after salt spray higher than bare steel (−0.96 V). The I_{corr} and corrosion rate were increased after salt spray which is a clear sign of the dispersal of the corrosive elements. However it should be noted that there is no substantial increase in I_{corr} and corrosion rate indicating the corrosion protection behaviour of the coating in saline environment.

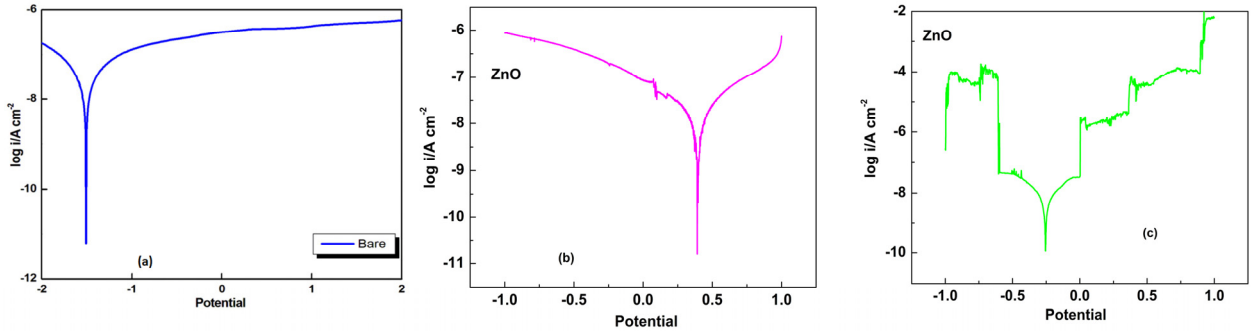

Figure 4. Polarization curve of ZnO coated stainless steel: (a) bare steel after salt spray; (b) before salt spray test; (c) after salt spray test.

Table 1. Electrochemical potential dynamic polarization parameters for SS 304L coated with ZnO.

ZnO	E_{corr} (V)	I_{corr} (μA)	β_a (mv)	β_c (mv)	CR (mmpy)
before salt spray	0.41	0.012	320.6	396.9	79.06×10^{-6}
after salt spray	−0.25	0.017	256.5	210.4	135.17×10^{-3}

3.4. EIS studies

The EIS curves of zinc oxide thin film deposited on stainless steel former and later to salt spray test is depicted in the Figures 5a, b respectively. The impedance parameters for thin film coated on steel specimen were estimated by matching the data with an equivalent circuit using Biologic science instruments circuits and the corresponding circuit of the ZnO layered stainless steel substrate is depicted in the Figure 6. R_s represent uncompensated solution resistance, whereas R_p and R_{ct} represent pore resistance and charge transfer resistance respectively. The pore capacitance, double layer capacitance and Warburg diffusion were represented by C_p, C_d and W respectively. These values were estimated by fitting the data with equivalent circuit and are shown in the Table 2.

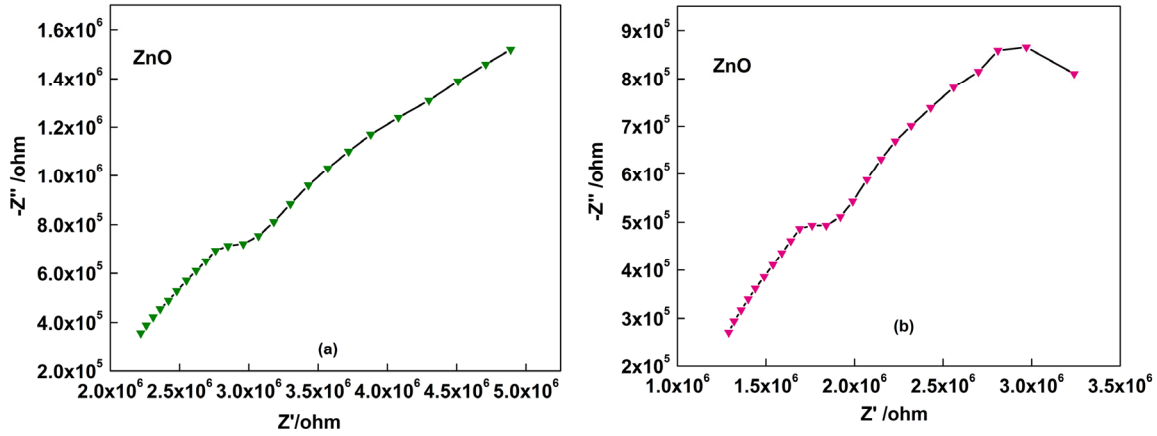

Figure 5. Nyquist plot of ZnO coated stainless steel: (a) before salt spray test; (b) after salt spray test.

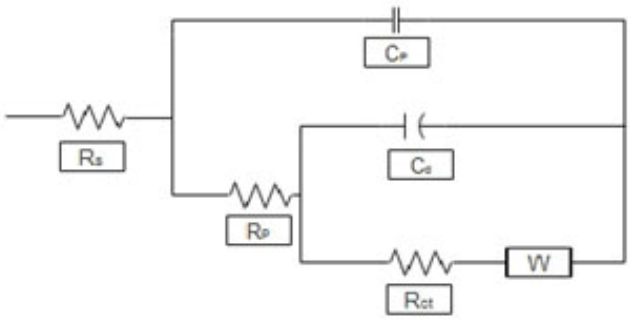

Figure 6. Equivalent circuit of ZnO coated stainless steel substrates.

Table 2. Parameters of the equivalent circuit shown in Figure 6.

ZnO	Rs	Cp	Rp	Cd	Rct	W	
						Rd3	td3
Before Salt Spray	2.11×10^6 Ω	4.95×10^{-9} F	1.007×10^6 Ω	16.31×10^{-9} F	856046 Ω	1.9992×10^6	0.2266 S
After Salt Spray	1.17×10^6 Ω	5.66×10^{-9} F	641497 Ω	17.33×10^{-9} F	443690 Ω	1.338×10^6	0.2016 S

In low and high frequency regions, the Warburg diffusion process is dominant as evident from the straight line nature [39]. However in the mid frequency regions, a semicircle can be observed. The observation of semi circle indicates that transfer resistance determines the impedance in this region. From the Figure 5b, it can be observed that transfer resistance is dominant in low and high frequency regions compared to that of the sample before salt spray. The corrosion resistance of bare steel is 72 kΩ [40]. The R_{ct} values calculated for ZnO coated thin films before and after salt spray are 856 kΩ and 443 kΩ. The decrease in corrosion resistance on salt spray may be attributed to the presence of aggressive environment.

The variation of the impedance with frequency of the ZnO thin film coated on stainless steel former and later corrosion test is depicted in the Figures 7a, b respectively. It can be observed that there is no appreciable change in the spectra which reveals the strength and durability of the thin film coating in the brackish environment.

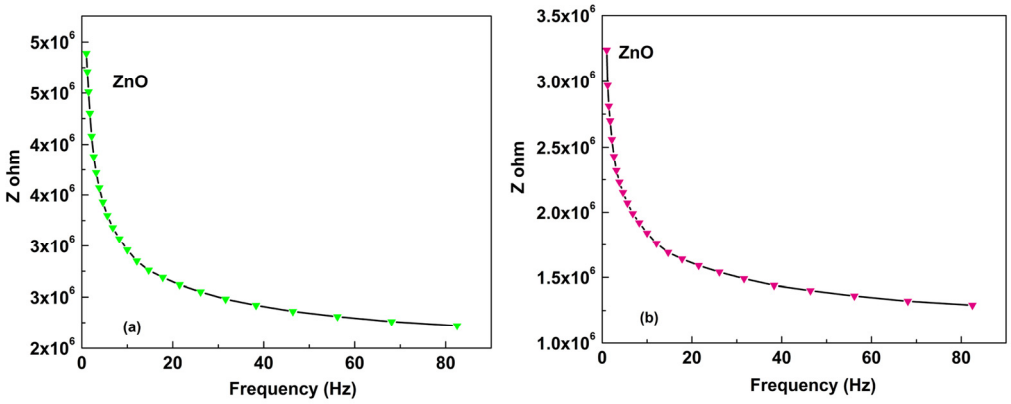

Figure 7. Impedance spectra of ZnO coated stainless steel: (a) before salt spray test; (b) after salt spray test.

3.5. Open circuit potential studies

The variation of OCP with time for ZnO thin film is depicted in the Figures 8a, b respectively. It is seen that the OCP value increases with time indicating thermodynamic stability of the coated samples (before salt spray test against corrosion). The OCP value decreases around 280 hours after salt spray indicating decrease in passivation capacity.

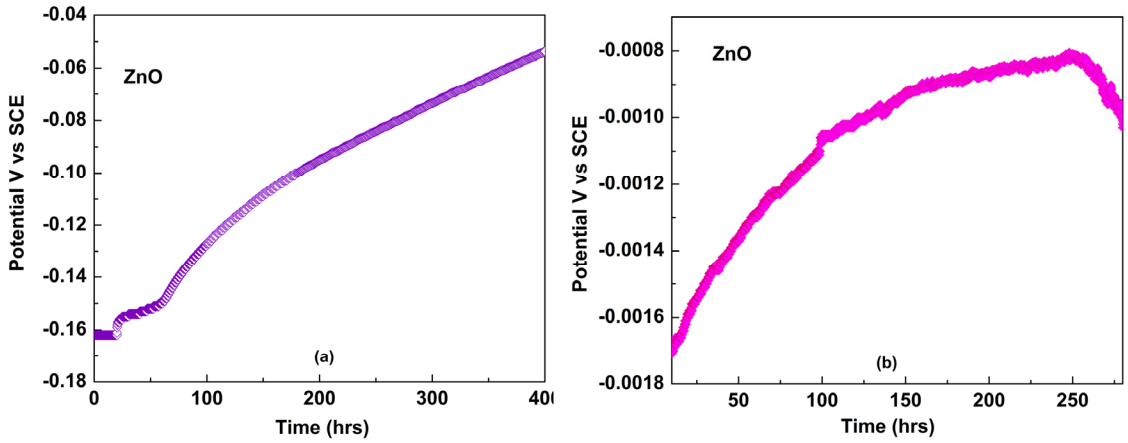

Figure 8. OCP Variation of ZnO coated stainless steel: (a) before salt spray test; (b) after salt spray test.

3.6. Salt spray test

The exclusive industrial method to test the anticorrosion behavior of the zinc oxide thin films was to conduct neutral salt spray test. The bare SS 304L after 390 h salt spray test is shown in the Figure 9. The nanostructured ZnO coating after salt treatment is shown in the Figure 10. This test asses the porous free nature of the deposited zinc oxide thin film. The intentional vulnerable environment produced by the salt spray did not reduce the performance, durability and the lifetime of coatings. No peel off or blistering observed in the coated area which indicated the adherence and porous nature of the coatings in the splash zone. The salt spray corrosion test confirms that the present coating was an effective protection against corrosion with this low cost profile.

Figure 9. Bare SS 304L after 390 h salt spray test.

Figure10. ZnO thin films after 390 h salt spray test.

3.7. AFM assisted Nanoindentation studies

The morphology of the zinc oxide thin film grown on the steel substrate was analyzed using AFM studies. The AFM images of the samples before and after nanoindentation are shown in the Figure 11. From the figures, it can be observed that there were no cracks or blisters after indentation that reiterates the adherence of the coating. The AFM images of zinc oxide layer former and later nanoindentation (after salt treatment for 390 h) are shown in the Figure 12. The films remained stable and adherent followed by aggressive salt treatment that shows the present coating is suitable for applications in marine environment. The surface roughness values (RMS deviation and arithmetic mean deviation) were calculated from the AFM analysis and are showed in the Table 3. The surface roughness values of the deposited films did not show significant variation on nanoindentation which authenticates the high adhesive nature of the coated thin film.

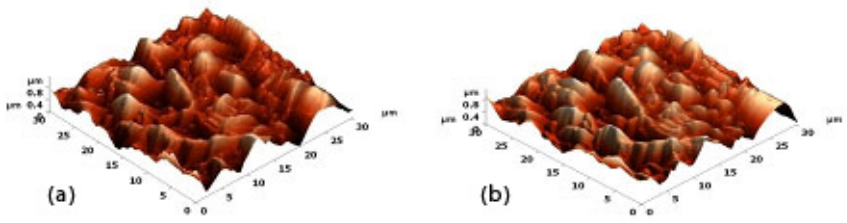

Figure 11. AFM images of as coated ZnO thin films: (a) before nanoindendation; and (b) after nanoindentation.

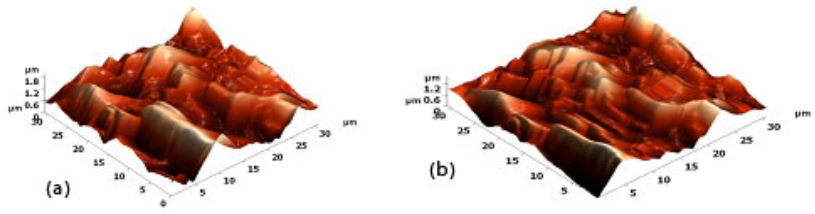

Figure 12. AFM images of ZnO thin films after salt spray: (a) before nanoindendation; and (b) after nanoindentation.

Table 3. Root mean square deviation (R_q) and Arithmetical mean deviation (R_a) of surface roughness values for coated films.

Sample	Before nanoindentation		After nanoindentation	
	R_q (nm)	R_a (nm)	R_q (nm)	R_a (nm)
As coated ZnO	227	221	223	217
ZnO after salt spray	224	217	221	212

Nanoindentation techniques examine the mechanical behaviour of exceptionally small configuration. The typical indentation plots of load versus depth of penetration at a maximum load of 8000 mN and 5000 mN for the spray coated zinc oxide thin films earlier and later salt spray corrosion test are depicted in Figure 13a,b respectively. There were no discontinuities or "pop-in" events in the indentation plot indicating the stability of the deposited film [41,42]. The depth of penetration before salt spray test is 520 nm under the load of 8000 mN that is found to decrease up to 375 nm under the load of 5000 mN after neutral salt spray test which can be ascribed to the reduced toughness of the film due to the action of 390 h of salt environment. The slight ruggedness is observed in the plot which may be attributed to the natural disturbances which is common in extremely small indentation process.

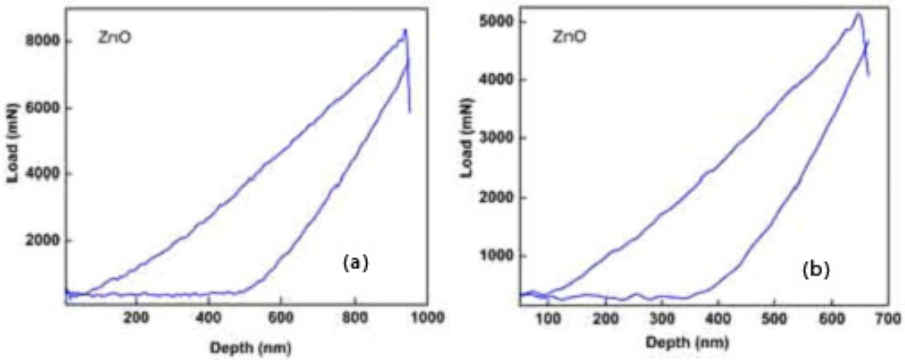

Figure 13. Hardness test for ZnO before and after corrosion test: (a) before salt spray test; (b) after salt spray test.

4. Conclusion

The nanostructured ZnO thin films were synthesized using spray coating of nanoparticles of ZnO on steel specimen. The FESEM study of the ZnO thin films indicates that grain size in nanometers was conserved on coating. The EDAX pattern indicates that the peaks corresponding to Zn and O only are found in the prepared thin film. The peaks observed in the photoluminescence spectrum show excitonic and defect level emissions. The positive shift of equilibrium corrosion potential in the tafel studies of zinc oxide coated stainless steel reveals the increase of corrosion resistance in saline environment. The electrochemical impedance spectroscopy reveals that the charge transfer resistance and ion diffusion rate are high compared to bare steel later which followed by salt treatment. The photograph of thin films later corrosion test confirms that there was no peeling off or blistering in the coated area which indicates the adherence of the coatings. The AFM images

reveals that the surface roughness values of the deposited films did not show considerable variation on nanoindentation which authenticates the high adhesive nature of the deposited thin film.

Acknowledgement

The authors acknowledge Optoelectroctronics Department, University of Kerala, Thiruvananthapuram, Kerala, for providing FESEM, EDAX, Micro-Raman facilities at a concessional rate. The authors are thankful to Dr. R. Yamuna, Associate Professor, Department of Sciences, Amrita School of Engineering, Coimbatore, Tamil Nadu, for their help in recording TAFEL, EIS and OCP measurements. The authors also acknowledge Roots Industries Pvt Ltd, Coimbatore, for performing salt spray corrosion test at a concessional rate.

Conflict of interest

All authors declare no conflicts of interest in this paper.

References

1. Lander JJ (1960) Solids Reactions of Lithium as a donor and an acceptor in ZnO. *J Phys Chem Solid* 15: 324–334.
2. Joshi RN, Singh VP, Mcclure JC (1995) Characteristics of indium tin oxide films deposited by r.f. magnetron sputtering. *Thin Solid Films* 257: 32–35.
3. Ronovich JA, Golmoya D, Bube RH (1980) Photovoltaic properties of ZnO/CdTe heterojunctions prepared by spray pyrolysis. *J Appl Phys* 51: 4260–4268.
4. Nunesa P, Fernandesa B, Fortunatoa E, et al. (1999) Performances presented by zinc oxide thin films deposited by spray pyrolysis. *Thin Solid Films* 337: 176–179.
5. Fantini M, Torriani I (1986) The compositional and structural properties of sprayed SnO2:F thin films. *Thin Solid Films* 138: 255–265.
6. Chopra KL, Major S, Panday DK (1983) Transparent conductors—a status review. *Thin Solid Films* 102: 1–46.
7. Han MY, Jou JH (1995) Determination of the mechanical properties of r.f-magnetron-sputtered ZnO thin films on substrates. *Thin Solid Films* 260: 58–64.
8. Lia ZW, Gao W, Reeves RJ (2005) Zinc oxide films by thermal oxidation of zinc thin films. *Surf Coat Technol* 198: 319–323.
9. Ashour A, Kaid MA, El-Sayed NZ, et al. (2006) Physical properties of ZnO thin films deposited by spray pyrolysis technique. *Appl Surf Sci* 252: 7844–7848.
10. Wang Y, Wang W, Liu Y, et al. (2011) Study of localized corrosion of 304 stainless steel under chloride solution droplets using the wire beam electrode. *Corros Sci* 53: 2963–2968.
11. Kumagai H, Matsumoto M, Toyoda K, et al. (1994) Fabrication of Multilayers with Growth Controlled by Sequential Surface Chemical Reactions. *Jap J Appl Phys* 33: 7086–7089.
12. Hu Q, Zhang G, Qju Y, et al. (2011) The crevice corrosion behaviour of stainless steel in sodium chloride solution. *Corros Sci* 53: 4065–4072.
13. Shajudheen VPM, Rani KA, Kumar VS, et al. (2018) Optical and corrosion studies of spray pyrolysis coated titanium dioxide thin films. *Adv Sci Lett* 24: 5836–5842.

14. Radhakrishnan S, Siju CR, Mahanta D, et al. (2009) Conducting polyaniline-nano-TiO_2 composites for smart corrosion resistant coatings. *Electrochim Acta* 54: 1249–1254.
15. Zheludkevich ML, Tedim J, Ferreira NGS (2012) Smart coatings for active corrosion protection based on multi-functional micro and nano containers. *Electrochim Acta* 82: 314–323.
16. Oglek K, Morel S, Jacquet D (2006) Observation of self-healing hunctions on the cut edge of galvanized steel using SVET and pH microscopy. *J Electrochem Soc* 153: B1–B5.
17. TamilSelvi S, Raman V, Rajendran N (2003) Corrosion inhibition of mild steel by benzotriazole derivatives in acidic medium. *J Appl Electrochem* 33: 1175–1182.
18. Praveen BM, Venkatesha TV, Arthoba NY, et al. (2007) Corrosion studies of carbon nanotubes—Zn composite coating. *Sur Coat Technol* 201: 5836–5842.
19. Benena L, Bonora PL, Borello A, et al. (2002) Wear corrosion properties of nano-structured SiC-nickel composite coatings obtained by electroplating. *Wear* 249: 995–1003.
20. Zimmerman AF, Palumbo G, Aust KT, et al. (2002) Mechanical properties of nickel silicon carbide nanocomposites. *Mater Sci Eng A* 328: 137–146.
21. Schuler T, Aegerter MA (1999) Optical, electrical and structural properties of sol gel ZnO:Al coatings. *Thin Solid Films* 351: 125–131.
22. Bagnall DM, Chen YF, Zhu Z, et al. (1997) Optically pumped lasing of ZnO at room temperature. *Appl Phys Lett* 70: 2230–2232.
23. Ellmer K, Wendt R (1997) D.c. and r.f. (reactive) magnetron sputtering of ZnO:Al films from metallic and ceramic targets: A comparative study. *Surf Coat Technol* 93: 21–26.
24. Fiddes AJC, Durose K, Brinkman AW, et al. (1996) Preparation of ZnO films by spray pyrolysis. *J Cryst Growth* 159: 210–213.
25. Ryu YR, Zhu S, Budai JD, et al. (2000) Optical and structural properties of ZnO films deposited on GaAs by pulsed laser deposition. *J Appl Phys* 88: 201–204.
26. Bethke S, Pan H, Wessels BW (1988) Luminescence of heteroepitaxial zinc oxide. *Appl Phys Lett* 52: 138–142.
27. Cho S, Ma J, Kim Y, et al. (1999) Photoluminescence and ultraviolet lasing of polycrystalline ZnO thin films prepared by the oxidation of the metallic Zn. *Appl Phys Lett* 75: 2761–2763.
28. Benny J, Gopchandran KG, Thomas PV, et al. (1999) A study on the chemical spray deposition of zinc oxide thin films and their structural and electrical properties. *Mater Chem Phys* 58: 71–77.
29. Manesh HD, Taheri AK (2003) Bond strength and formability of an aluminum-clad steel sheet. *J Alloys Compd* 361: 138–143.
30. Zhang QB, Hua YX (2009) Corrosion inhibition of mild steel by alkylimidazolium ionic liquids in hydrochloric acid. *Electrochim Acta* 54: 1881–1887.
31. Chiew SP, Zhao MS, Lee CK (2014) Mechanical properties of heat-treated high strength steel under fire/post-fire conditions. *J Constr Steel Res* 98: 12–19.
32. Dan L, Feigaox XU, Shao L, et al. (2015) Effect of the addition of 3-glycidoxypropyltrimethoxysilane to tetraethoxyorthosilicate-based stone protective coating using n-octylamine as a catalyst. *Bull Mater Sci* 38: 49–55.
33. Zhao H, Yu M, Liu J, et al. (2015) Effect of Surface Roughness on Corrosion Resistance of Sol-Gel Coatings on AA2024-T3 Alloy. *J Electrochem Soc* 162: C718–C724.
34. Shajudheen MVP, Rani AK, Kumar SV, et al. (2016) Low temperature synthesis of Zinc Oxide nanoparticles and their characterization. *Adv Phys Lett* 3: 19–23.

35. Arthoba NY, Venkatesha TV (2005) A new condensation product for zinc plating from non-cyanide alkaline bath. *Bull Mater Sci* 28: 495–501.
36. Liu YX, Liu YC, Shao CL, et al. (2004) Excitonic properties of ZnO nanocrystalline films prepared by oxidation of zinc-implanted silica. *J Phys D: Appl Phys* 37: 3025–3029.
37. Ramanathan S, Patibandla S, Bandyopadhyay S, et al. (2006) Fluorescence and infrared spectroscopy of electrochemically self assembled ZnO nanowires: Evidence of the quantum confined Stark effect. *J Mater Sci Mater Electron* 17: 651–655.
38. Hosseini MG, Bagheri R, Najjar R (2011) Electropolymerization of Polypyrrole and Polypyrrole-ZnO nanocomposites on mild steel and its corrosion protection performance. *J Appl Polym Sci* 121: 3159–3166.
39. Huang H, Tian J, Zhang WK, et al. (2011) Electrochromic properties of porous NiO thin film as a counter electrode for NiO/WO3 complementary electrochromic window. *Electrochim Acta* 56: 4281–4286.
40. Shan CX, Hou X, Choy KL (2008) Corrosion resistance of TiO_2 films grown on stainless steel by atomic layer deposition. *Surf Coat Technol* 202: 2399–2402.
41. Muhamed SVP, Saravana KS, Senthil KV, et al. (2018) Investigation of anticorrosion properties of nanocomposites of spray coated zinc oxide and titanium dioxide thin films on stainless steel (304L SS) in saline environment. *Mater Res Express* 5: 1–11.
42. Christopher AS (2006) Nanoindentation studies of materials. *Mater Today* 9: 32–40.

AIMS Press